

Delaying or advancing higher-order sideband signals with active optomechanics

Yafeng Jiao^{1,2†}, Hao Lü^{3,4†}, Jun Qian^{3,*}, Yong Li², and H. Jing^{1,3,5*}

¹Department of Physics, Henan Normal University, Xinxiang 453007, China

²Beijing Computational Science Research Center, Beijing 100084, China

³Key Laboratory for Quantum Optics, Shanghai Institute of Optics and Fine Mechanics, Chinese Academy of Science, Shanghai 201800, China

⁴University of Chinese Academy of Sciences, Beijing 100049, China

⁵Synergetic Innovation Center for Quantum Effects and Applications, Hunan Normal University, Changsha 410081, China

* jqian@siom.ac.cn, jinghui73@foxmail.com

† These authors contributed equally to this work.

Abstract: We study the gain-assisted light transmissions in optomechanical systems, especially the nonlinear higher-order sideband process. We find that: (i) in a single active cavity, the efficiency of the second-order process is considerably enhanced, and the accompanying group delay can surpass that of the probe field, which is unattainable for a lossy cavity (i.e. without any gain); (ii) in an active-passive compound system, the second-order process can be further enhanced by approaching to the gain-loss balance, and hundreds of microsecond of relative delay or advance are achievable between the probe and the second-order signal, indicating an active optomechanical modulator both in frequency and time domains.

© 2024 Optical Society of America

OCIS codes: (270.1670) Coherent optical effect; (140.3945) Microcavities

References and links

1. T. J. Kippenberg and K. J. Vahala, *Cavity optomechanics: Back-action at the mesoscale*, *Science* **321**, 1172-1176 (2008).
2. F. Marquardt and S. M. Girvin, *Optomechanics*, *Physics* **2**, 40 (2009).
3. M. Aspelmeyer, P. Meystre, and K. Schwab, *Quantum optomechanics*, *Phys. Today* **65**, 29-35 (2012).
4. M. Metcalfe, *Applications of cavity optomechanics*, *App. Phys. Rev.* **1**, 031105 (2014).
5. J. M. Dobrindt, I. Wilson-Rae, and T. J. Kippenberg, *Parametric normal-mode splitting in cavity optomechanics*, *Phys. Rev. Lett.* **101**, 263602 (2008).
6. S. Gröblacher, K. Hammerer, M. R. Vanner, and M. Aspelmeyer, *Observation of strong coupling between a micromechanical resonator and an optical cavity field*, *Nature (London)* **460**, 724-727 (2009).
7. O. Arcizet, P. -F. Cohadon, T. Briant, M. Pinard, A. Heidmann, J.-M. Mackowski, C. Michel, L. Pinard, O. Français, and L. Rousseau, *High-sensitivity optical monitoring of a micromechanical resonator with a quantum-limited optomechanical sensor*, *Phys. Rev. Lett.* **97**, 133601 (2006).
8. J. D. Teufel, T. Donner, M. A. Castellanos-Beltran, J. W. Harlow, and K. W. Lehnert, *Nanomechanical motion measured with an imprecision below that at the standard quantum limit*, *Nat. Nanotechnol.* **4**, 820-823 (2009).
9. J. D. Teufel, T. Donner, D. Li, J. W. Harlow, M. S. Allman, K. Cicak, A. J. Sirois, J. D. Whittaker, K. W. Lehnert, and R. W. Simmonds, *Sideband cooling of micromechanical motion to the quantum ground state*, *Nature (London)* **475**, 359-363 (2011).
10. J. Chan, T. P. Mayer Alegre, A. H. Safavi-Naeini, J. T. Hill, A. Krause, S. Gröblacher, M. Aspelmeyer, and O. Painter, *Laser cooling of a nanomechanical oscillator into its quantum ground state*, *Nature (London)* **478**, 89-92 (2011).

11. I. S. Grudinin, H. Lee, O. Painter, and K. J. Vahala, *Phonon laser action in a tunable two-level system*, Phys. Rev. Lett. **104**, 083901 (2010).
12. H. Jing, S. K. Özdemir, X.-Y. Lü, J. Zhang, L. Yang, and F. Nori, *PT-symmetric phonon laser*, Phys. Rev. Lett. **113**, 053604 (2014).
13. W. Z. Jia and Z. D. Wang, *Single-photon transport in a one-dimensional waveguide coupling to a hybrid atom-optomechanical system*, Phys. Rev. A, **88**, 063821 (2013).
14. E. E. Wollman, C. U. Lei, A. J. Weinstein, J. Suh, A. Kronwald, F. Marquardt, A. A. Clerk, and K. C. Schwab, *Quantum squeezing of motion in a mechanical resonator*, Science **349**,952-955 (2015)
15. K.-J. Boller, A. Imamoglu, and S. E. Harris, *Observation of electromagnetically induced transparency*, Phys. Rev. Lett. **66**, 2593 (1991).
16. M. D. Lukin, M. Fleischhauer, M. O. Scully, and V. L. Velichansky, *Intracavity electromagnetically induced transparency*, Opt. Lett. **23**, 295-297 (1998).
17. M. Fleischhauer, A. Imamoglu, and J. P. Marangos, *Electromagnetically induced transparency: Optics in coherent media*, Rev. Mod. Phys. **77**, 633-673 (2005).
18. G. S. Agarwal and S. Huang, *Electromagnetically induced transparency in mechanical effects of light*, Phys. Rev. A, **81**, 041803 (2010).
19. S. Weis, R. Rivière, S. Deleglise, E. Gavartin, O. Arcizet, A. Schliesser, and T. J. Kippenberg, *Optomechanically induced transparency*, Science, **330**,1520-1523 (2010).
20. A. H. Safavi-Naeini, T. P. M. Alegre, J. Chan, M. Eichenfield, M. Winger, Q. Lin, J. T. Hill, D. E. Chang, and O. Painter, *Electromagnetically induced transparency and slow light with optomechanics*, Nature **472**, 69-73 (2011).
21. X. Zhou, F. Hocke, A. Schliesser, A. Marx, H. Huebl, R. Gross, and T. J. Kippenberg, *Slowing, advancing and switching of microwave signals using circuit nanoelectromechanics*, Nat. Phys. **9**,179-184 (2013).
22. D. E. Chang, A. H. Safavi-Naeini, M. Hafezi, and O. Painter, *Slowing and stopping light using an optomechanical crystal array*, New J. Phys. **13**,023003 (2011).
23. V. Fiore, Y. Yang, M. C. Kuzyk, R. Barbour, L. Tian, and H. Wang, *Storing optical information as a mechanical excitation in a silica optomechanical resonator*, Phys. Rev. Lett. **107**, 133601 (2011).
24. L. Fan, K. Y. Fong, M. Poot, and H. X. Tang, *Cascaded optical transparency in multimode-cavity optomechanical systems*, Nat. Commun. **6**, 5850 (2015).
25. K. Stannigel, P. Komar, S. J. M. Habraken, S. D. Bennett, M. D. Lukin, P. Zoller, and P. Rabl, *Optomechanical quantum information processing with photons and phonons*, Phys. Rev. Lett. **109**, 013603 (2012).
26. M. Ludwig, A. H. Safavi-Naeini, O. Painter, and F. Marquardt, *Enhanced quantum nonlinearities in a two-mode optomechanical system*, Phys. Rev. Lett. **109**, 063601 (2012).
27. S. Basiri-Esfahani, U. Akram, and G. J. Milburn, *Phonon number measurements using single photon optomechanics*. New J. Phys. **14**,085017 (2012).
28. K. Stannigel, P. Rabl, A. S. Sørensen, M. D. Lukin, and P. Zoller, *Optomechanical transducers for quantum information processing*, Phys. Rev. A **84**, 042341 (2011).
29. A. Nunnenkamp, K. Børkje, and S. M. Girvin, *Single-photon optomechanics*, Phys. Rev. Lett. **107**, 063602 (2011).
30. H. Xiong, L.-G. Si, A. -S. Zheng, X. Yang, and Y. Wu, *Higher-order sidebands in optomechanically induced transparency*, Phys. Rev. A **86**, 013815 (2012).
31. M.-A. Lemonde, N. Didier, and A. A. Clerk, *Nonlinear interaction effects in a strongly driven optomechanical cavity*, Phys. Rev. Lett. **111**, 053602 (2013).
32. K. Børkje, A. Nunnenkamp, J. D. Teufel, and S. M. Girvin, *Signatures of nonlinear cavity optomechanics in the weak coupling regime*, Phys. Rev. Lett. **111**, 053603 (2013).
33. Y. -C. Liu, Y. -F. Xiao, Y. -L. Chen, X. -C. Yu, and Q. Gong, *Parametric down-conversion and polariton pair generation in optomechanical systems*, Phys. Rev. Lett. **111**, 083601 (2013).
34. A. Kronwald, and F. Marquardt, *Optomechanically Induced Transparency in the Nonlinear Quantum Regime*, Phys. Rev. Lett. **111**, 133601 (2013).
35. J. Ma, C. You, L.-G. Si, H. Xiong, J. Li, X. Yang, and Y. Wu, *Optomechanically induced transparency in the presence of an external time-harmonic-driving force*, Sci. Rep. **5**, 11278 (2015).
36. H. Suzuki, and E. Brown, and R. Sterling, *Nonlinear dynamics of an optomechanical system with a coherent mechanical pump: second-order sideband generation*, Phys. Rev. A **92**, 033823 (2015).
37. P.-C. Ma, J.-Q. Zhang, Y. Xiao, M. Feng, and Z.-M. Zhang, *Tunable double optomechanically induced transparency in an optomechanical system*, Phys. Rev. A **90**, 043825 (2014).
38. C. M. Bender, and S. Boettcher, *Real spectra in non-Hermitian Hamiltonians having PT symmetry*, Phys. Rev. Lett. **80**, 5243 (1998).
39. C. M. Bender, M. Gianfreda, S. K. Özdemir, B. Peng, and L. Yang, *Twofold transition in PT-symmetric coupled oscillators*, Phys. Rev. A **88**, 062111 (2013).
40. B. Peng, S. K. Özdemir, F. Lei, F. Monifi, M. Gianfreda, G. L. Long, S. Fan, F. Nori, C. M. Bender, and L. Yang, *Parity-time-symmetric whispering-gallery microcavities*, Nat. Phys. **10**, 394-398 (2014).
41. L. Chang, X. Jiang, S. Hua, C. Yang, J. Wen, L. Jiang, G. Li, G. Wang, and M. Xiao, *Parity-time symmetry and variable optical isolation in active-passive-coupled microresonators*, Nat. Photon. **8**, 524-529 (2014).

42. L. Feng, Z. J. Wong, R.-M. Ma, Y. Wang, and X. Zhang, *Single-mode laser by parity-time symmetry breaking*, *Science* **346**, 972-975 (2014).
 43. H. Hodaei, M.-A. Miri, M. Heinrich, D. N. Christodoulides, and M. Khajavikhan, *Parity-time -symmetric microring lasers*, *Science* **346**, 975-978 (2014).
 44. B. Peng, S. K. Özdemir, S. Rotter, H. Yilmaz, M. Liertzer, F. Monifi, C. M. Bender, F. Nori, and L. Yang, *Loss-induced suppression and revival of lasing*, *Science* **346**, 328-332 (2014).
 45. W. Wan, Y. Chong, L. Ge, H. Noh, A. D. Stone, and H. Cao, *Time-reversed lasing and interferometric control of absorption*, *Science* **331**, 889 (2011).
 46. X.-Y. Lü, H. Jing, J.-Y. Ma, and Y. Wu, *PT-symmetry-breaking chaos in optomechanics*, *Phys. Rev. Lett.* **114**, 253601 (2015).
 47. H. Jing, S. K. Özdemir, Z. Geng, J. Zhang, X. Y. Lü, B. Peng, L. Yang, and F. Nori, *Optomechanically-induced transparency in parity-time-symmetric microresonators*, *Sci. Rep.* **5**, 9663 (2015).
 48. T. Oishi and M. Tomita, *Inverted coupled-resonator-induced transparency*, *Phys. Rev. A* **88**, 013813 (2013).
 49. L. Ge, S. Faez, F. Marquardt, and H. E. Türeci, *Gain-tunable optomechanical cooling in a laser cavity*, *Phys. Rev. A* **87**, 053839 (2013).
 50. W. Z. Jia, L. F. Wei, Y. Li, and Y. X. Liu, *Phase-dependent optical response properties in an optomechanical system by coherently driving the mechanical resonator*, *Phys. Rev. A* **91**, 043843 (2015).
-

1. Introduction

Cavity optomechanics (COM) or radiation-pressure-induced coherent photon-phonon coupling have led to a variety of important advances with practical values [1–4], including ultra-sensitive weak-force measurement [5–8], mechanical ground-state cooling [9, 10], phonon lasing [11, 12], single-photon transporting [13], and quantum squeezing of mechanical motion [14], to name a few of them. Among these achievements, optomechanically-induced transparency (OMIT), as an analogue of electromagnetically-induced transparency in atomic systems [15–17], was theoretically proposed [18] and experimentally demonstrated [19, 20], providing a new way to manipulate or store a laser light in a solid-state architecture [21–24]. In view of nonlinear nature of the optomechanical interaction, more exotic nonlinear processes and novel applications have also been revealed [25–27], e.g. single-photon COM [28, 29] and nonlinear OMIT [30–34]. As a prominent feature of nonlinear OMIT, the optical higher-order sideband was firstly predicted for a single passive cavity [30] and then extended to a COM system with a mechanical driving [35, 36] or an electrostatically coupled object [37].

In parallel with these advances, parity-time(PT)-symmetric phase transition [38, 39] has also been experimentally observed in coupled optical microresonators [40], opening up novel applications such as low-power optical diodes [40, 41], single-mode lasing [42, 43], loss-induced lasing [44], and lasing with perfect absorption [45]. Combining these two research fields, one can realize PT-symmetric hybrid devices with photons and phonons, exhibiting unconventional effects such as thresholdless phonon lasing [12] and PT-broken chaos [46]. An inverted OMIT spectrum, i.e. a non-amplifying dip in the otherwise strongly amplifying region, was also identified in the linear process for such a PT-symmetric system [47] (for a purely optical experiment on the similar effect, see Ref. [48]).

Inspired by the works mentioned above, here we study the nonlinear OMIT process and particularly the higher-order sidebands in a single active cavity or a compound device with active-passive resonators. We show that (i) the second-order sideband exhibits an inverted-OMIT profile in both a single cavity and a compound device, which is similar to that as observed in the linear transmission rate [47]; (ii) the transmission of the second-order sideband pulse can be significantly enhanced in the vicinity of gain-loss balance; (iii) the group delays of both first-order and second-order sideband pulses show a strong dependence on the optical pump power, and their relative delay or advance can be well adjusted within several hundreds of microsecond. These features indicate potential applications of active COM devices in controlling light transmissions both in frequency and time domains. We note that the group delay of the second-order sideband and the tunable relative delay or advance between different sideband pulses have

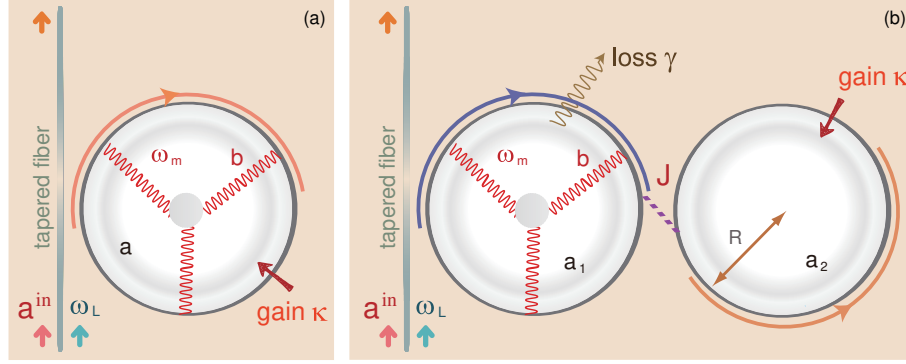


Fig. 1. (Color online) Schematic of COM in a single active cavity (a) or an active-passive compound structure (b). In (b), the left cavity with an optical decay rate γ is coupled with a tapered fiber, and the right cavity with an optical gain κ [40, 47] is coupled to the left cavity with an optical tunneling rate J . In both cases, only the cavity coupled to the fiber supports a mechanical mode at frequency ω_m and is driven by a pump field at frequency ω_L .

not been investigated in previous literatures.

This paper is organized as follows. In Sec. 2, we present the OMIT models for both a single active cavity and an active-passive compound system, with which to calculate the optical spectral responses and the associated group delays of both the probe field and the second-order sideband. Then in Sec. 3, we analyze in details the results of optical transmissions rates and group delays in a single cavity or an active-passive compound system, respectively, focusing on the important roles of the pump power and the gain-to-loss ratio. Finally in Sec. 4, we conclude with a brief discussion of the results presented in this work and an outlook of our future works.

2. Theoretical Model

As shown in Fig. 1, for possible comparisons, we consider two different setups consisting of a single active optomechanical cavity [49] and an active-passive compound structure, respectively. In both cases, the cavity-mode resonance frequency is ω_c , the cavity coupled with the tapered fiber contains a mechanical mode (with the effective mass m and the damping rate Γ_m) [11], and the COM coupling strength is denoted by g . As in Ref. [40], the active resonator, fabricated from Er^{3+} -doped silica, can emit photons in the 1550nm band, when driven by a laser in the 980nm or 1450nm bands. In Fig. 1(a), we first focus on the gain-assisted OMIT in a single cavity, including the second-order transmission rate and the associated group delay. In Fig. 1(b), we turn to study the enhancement of the second-order sideband in the vicinity of gain-loss balance in a compound structure. Note that only the photons at the emission band of 1550nm can tunnel through the air gap between the resonators, which provides an optical gain κ to compensate the optical loss γ in the passive resonator [40]. To observe the OMIT phenomenon, the optomechanical cavity is driven by both a strong pump laser at frequency ω_l and a weak probe light at frequency ω_p , with the amplitudes

$$\varepsilon_l = \sqrt{\frac{2\gamma P_l}{\hbar\omega_l}}, \quad \varepsilon_p = \sqrt{\frac{2\gamma P_{in}}{\hbar\omega_p}},$$

respectively, where P_l and P_{in} denote the powers of the control and probe lasers. We are interested in the role of nonlinear COM interactions on the optical responses of the systems, par-

ticularly the relative group delay or advance of the probe light and the higher-order sideband pulse.

2.1. Nonlinear OMIT in a single active cavity

As illustrated in Fig. 1(a), we study the transmission rates of the probe field and the second-order sideband in a single active optomechanical cavity [49]. The Hamiltonian of the system can be written at the simplest level as

$$H_1 = \hbar\Delta_l a^\dagger a + \frac{p^2}{2m} + \frac{1}{2}m\omega_m^2 x^2 - \hbar g a^\dagger a x + i\hbar \left(\varepsilon_l a^\dagger + \varepsilon_p a^\dagger e^{-i\xi t} - h.c. \right), \quad (1)$$

with the optical operator a and the mechanical position or momentum operator x or p , and the cavity-pump detuning and the probe-pump detuning, respectively,

$$\Delta_l \equiv \omega_c - \omega_l, \quad \xi \equiv \omega_p - \omega_c.$$

The Heisenberg equations of motion of this system are then

$$\begin{aligned} \ddot{x} + \Gamma_m \dot{x} + \omega_m^2 x - \frac{\hbar g}{m} a^\dagger a &= 0, \\ \dot{a} + (i\Delta_l - igx - \kappa)a - \varepsilon_l &= \varepsilon_p e^{-i\xi t}. \end{aligned} \quad (2)$$

The optical or mechanical gain and damping terms are added phenomenologically into the Eq. (2) [12, 46]. Setting all the derivatives as zero leads to the steady-state values

$$x_s = \frac{\hbar g}{m\omega_m^2} |a_s|^2, \quad a_s = \frac{\varepsilon_l}{-\kappa + i\Delta_l - igx_s}. \quad (3)$$

All the operators are then divided into their stationary values and the remaining fluctuations, i.e. $x = x_s + \delta x$, $a = a_s + \delta a$, and the equations satisfied by the fluctuation terms are

$$\begin{aligned} \delta\ddot{x} + \Gamma_m \delta\dot{x} + \omega_m^2 \delta x - \frac{\hbar g}{m} (a_s \delta a^\dagger + a_s^* \delta a + \delta a^\dagger \delta a) &= 0, \\ \delta\dot{a} + (i\Delta_l - igx_s - \kappa) \delta a - ig(a_s \delta x + \delta x \delta a) &= 0. \end{aligned} \quad (4)$$

Here the second-order nonlinear terms such as $\delta x \delta a$ and $\delta a^\dagger \delta a$ are preserved in Eq. (4). Now we solve these equations by using the ansatz

$$\begin{aligned} \delta a &= A_+^{(1)} e^{-i\xi t} + A_-^{(1)} e^{i\xi t} + A_+^{(2)} e^{-2i\xi t} + A_-^{(2)} e^{2i\xi t}, \\ \delta x &= X^{(1)} e^{-i\xi t} + X^{(1)*} e^{i\xi t} + X^{(2)} e^{-2i\xi t} + X^{(2)*} e^{2i\xi t}, \end{aligned} \quad (5)$$

Substituting Eq. (5) into Eq. (4), and first neglecting the second-order parts in Eq. (5), leads to the linear response of the system

$$\begin{aligned} A_+^{(1)} &= \frac{[\lambda(\xi)\lambda_{s2}(\xi) + i\hbar g^2 |a_s|^2] \varepsilon_p}{\lambda(\xi)\lambda_{s1}(\xi)\lambda_{s2}(\xi) + i[\lambda_{s1}(\xi) - \lambda_{s2}(\xi)]\hbar g^2 |a_s|^2}, \\ X^{(1)} &= \frac{\lambda_{s2}(\xi)\hbar g a_s^* \varepsilon_p}{\lambda(\xi)\lambda_{s1}(\xi)\lambda_{s2}(\xi) + i[\lambda_{s1}(\xi) - \lambda_{s2}(\xi)]\hbar g^2 |a_s|^2}, \end{aligned} \quad (6)$$

where

$$\lambda(\xi) = m(\omega_m^2 - \xi^2 - i\xi\Gamma_m), \quad \lambda_{s1,s2}(\xi) = -i\xi - \kappa \pm (i\Delta_l - igx_s). \quad (7)$$

Combining Eqs. (4,5,6) gives the second-order sideband amplitude

$$A_+^{(2)} = \frac{-i\hbar g^4 a_s |a_s|^2 X^{(1)2} + [\hbar g^3 (\lambda_{s2}(2\xi) - \lambda_{s2}(\xi)) |a_s|^2 + ig \lambda_{s2}(\xi) \lambda(2\xi) \lambda_{s2}(2\xi)] A_+^{(1)} X^{(1)}}{\lambda_{s2}(\xi) [\lambda(2\xi) \lambda_{s1}(2\xi) \lambda_{s2}(2\xi) + i(\lambda_{s1}(2\xi) - \lambda_{s2}(2\xi)) \hbar g^2 |a_s|^2]} \quad (8)$$

We note that $A_+^{(2)}$, being proportional to ε_p^2 , is indeed smaller than the first-order term $A_+^{(1)}$ for a weak probe light. The first term or the second term of $A_+^{(2)}$ denotes an upconverted-like process of the pump light or the first-order sideband, respectively [30].

2.2. Nonlinear OMIT in active-passive-coupled resonators

Now we use the similar strategy as in the above derivations to treat the compound COM system as shown in Fig. 1(b). Including two optical modes $a_{1,2}$ and the mechanical mode containing now in the passive resonator, we write the Hamiltonian of this three-mode COM system as

$$H_2 = H_1 + \hbar \Delta_l a_2^\dagger a_2 - \hbar J (a_1^\dagger a_2 + a_2^\dagger a_1), \quad (9)$$

where for the expression of H_1 , we have used the replacement $a \rightarrow a_1$. The Heisenberg equations of this compound system are

$$\begin{aligned} \dot{x} &= -\Gamma_m \dot{x} - \omega_m^2 x - \frac{\hbar g}{m} a_1^\dagger a_1, \\ \dot{a}_1 &= (-i\Delta_l + igx - \gamma) a_1 + iJ a_2 + \varepsilon_l + \varepsilon_p e^{-i\xi t}, \\ \dot{a}_2 &= (-i\Delta_l + \kappa) a_2 + iJ a_1. \end{aligned} \quad (10)$$

Expanding the operators as follows

$$\begin{aligned} a_1 &= a_{1,s} + A_{1+}^{(1)} e^{-i\xi t} + A_{1-}^{(1)} e^{i\xi t} + A_{1+}^{(2)} e^{-2i\xi t} + A_{1-}^{(2)} e^{2i\xi t}, \\ a_2 &= a_{2,s} + A_{2+}^{(1)} e^{-i\xi t} + A_{2-}^{(1)} e^{i\xi t} + A_{2+}^{(2)} e^{-2i\xi t} + A_{2-}^{(2)} e^{2i\xi t}, \\ x &= x_s + X^{(1)} e^{-i\xi t} + X^{(1)*} e^{i\xi t} + X^{(2)} e^{-2i\xi t} + X^{(2)*} e^{2i\xi t}, \end{aligned} \quad (11)$$

where $a_{i,s}$ ($i = 1, 2$) and x_s denotes the steady values, leads to the amplitude of the first-order sideband $A_{1+}^{(1)}$ and $X^{(1)}$, as given in Ref. [47], and also the second-order sideband amplitude $A_{1+}^{(2)}$. We find that it has exactly the same form as the single-cavity result, i.e. the Eq. (8), but with the following replacements

$$a \rightarrow a_1, \quad A_+^{(1)} \rightarrow A_{1+}^{(1)}, \quad \lambda_{s1} \rightarrow \lambda_{d1}, \quad \lambda_{s2} \rightarrow \lambda_{d2}, \quad (12)$$

and

$$\lambda_{d1,d2}(\xi) \equiv -i\xi + \gamma \pm \left(i\Delta_l - igx_s + \frac{J^2}{i\Delta_l - i\xi - \kappa} \right). \quad (13)$$

In both cases, the expectation value of the output field can be obtained by using the standard input-output relation, i.e. $a_1^{out} = a_1^{in} - \sqrt{\gamma} a_1$, where a_1^{in} and a_1^{out} are the input and output field operators, respectively. The transmitted rate of the probe light [47] and the efficiency of the second-order sideband (i.e. the ratio of the amplitude of the output second-order sideband to the amplitude of the input probe light) [30] are then defined by

$$|t_p|^2 = \left| \frac{a_1^{out}}{a_1^{in}} \right|^2 = \left| 1 - \frac{\gamma}{\varepsilon_p} A_{1+}^{(1)} \right|^2, \quad \eta = \left| \frac{\gamma}{\varepsilon_p} A_{1+}^{(2)} \right|,$$

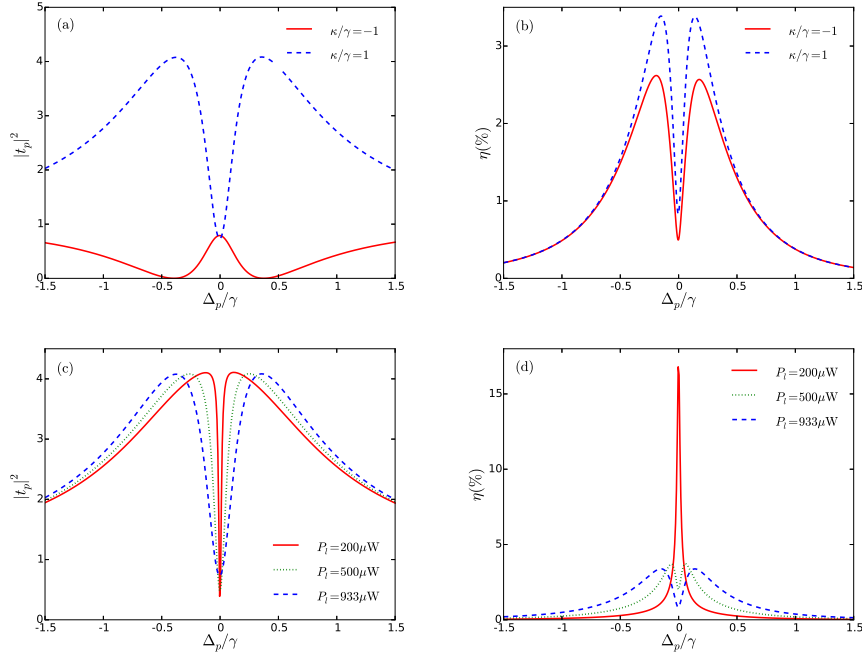


Fig. 2. Transmission of the probe light $|t_p|^2$ (a,c) and the efficiency of the second-order sideband process η (b,d) vary with the ratio κ/γ and the pump power P_l in the case of the single cavity. The pump power is fixed as $P_l = 933\mu\text{W}$ in (a) and (b), while $\kappa/\gamma = 1$ is chosen in (c) and (d).

respectively. In addition, the group delay of the probe light or the second-order sideband can be given by

$$\tau_g = \frac{d\arg(t_p)}{d\xi}\Big|_{\xi=\omega_m}, \quad \tau'_g = \frac{d\arg(A_{1+}^{(2)})}{d\omega}\Big|_{\xi=\omega_m} = \frac{d\arg(A_{1+}^{(2)})}{2d\xi}\Big|_{\xi=\omega_m},$$

respectively, taking into account of the second-order sideband frequency $\omega = 2\xi + \omega_l$. In the following, to illustrate the gain-assisted nonlinear OMIT effects, we choose the experimentally accessible parameters in our calculations, i.e. $\varepsilon_p/\varepsilon_l = 0.05$, (the radius of the resonators) $R = \omega_c/g = 34.5\mu\text{m}$, $m = 50\text{ ng}$, $\omega_c = 1.93 \times 10^5\text{ GHz}$, $\omega_m = 2\pi \times 23.4\text{ MHz}$, $\gamma = 6.43\text{ MHz}$ and $\Gamma_m = 2.4 \times 10^5\text{ kHz}$. We set $\Delta_l = \omega_c - \omega_l = \omega_m$ and then we have $\Delta_p \equiv \omega_p - \omega_c = \xi - \omega_m$. In the single cavity case, we compare the active OMIT and the familiar passive OMIT results, where a negative $\kappa < 0$ indicates a passive cavity; while in the double-resonator case, we focus on the different features of the second-order sideband in the PT-symmetric and the PT-broken regimes, by tuning the gain-to-loss ratio κ/γ .

3. Results and discussions

3.1. Single cavity with loss or gain

We first discuss the OMIT and second-order sideband in the single active-cavity configuration. Fig. 2 shows the results of $|t_p|^2$ and η as a function of Δ_p . For comparison, we also plot the results in a passive cavity [30]. We find that, in sharp contrast to the conventional OMIT profile in a lossy cavity, an inverted-OMIT profile is obviously visible for the probe field in an active cavity (see Fig. 2(a)), characterizing a non-amplifying dip in the otherwise strongly amplifying

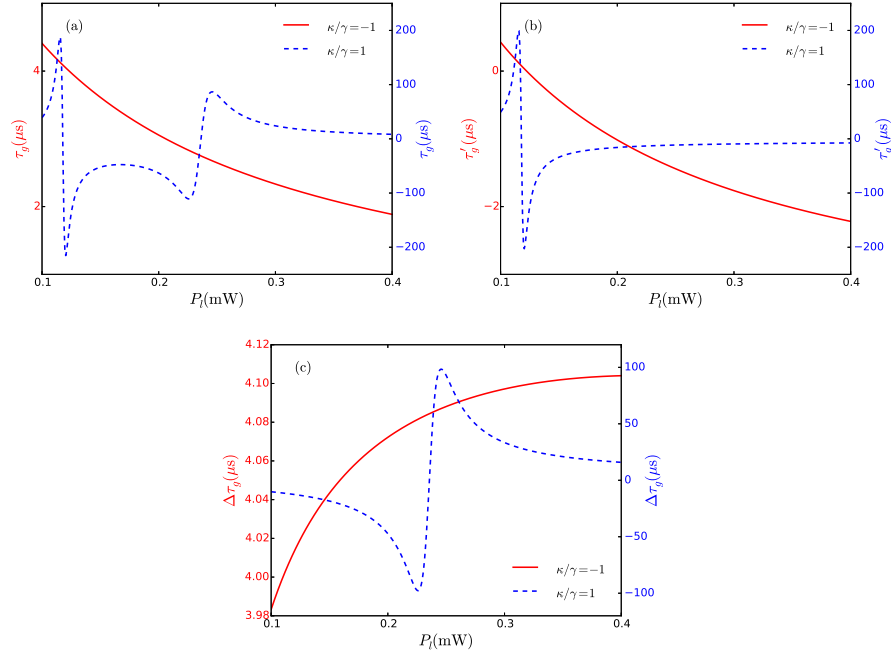


Fig. 3. Group delay or advance of the probe light (a) and the second-order sideband (b) at the resonance $\Delta_p = 0$, as a function of pump power for a single passive ($\kappa/\gamma = -1$) or an active cavity ($\kappa/\gamma = 1$). The relative group delay $\Delta\tau_g = \tau_g - \tau'_g$ is also shown in (c).

region. This feature was also observed in the active-passive compound system [47, 48]. However, this inverted feature does not exist in the second-order sideband process. As shown in Fig. 2(b), a double-peak structure in the transmission spectrum can be seen in both cases of passive and active COM systems. This indicates that by using an active cavity, one can simultaneously amplify the weak probe field and the sideband signal. This, again, is distinct from that in a passive COM system, where the generation of the second-order sideband tends to be suppressed in the transmission window of the probe field [30]. In Fig. 2(c,d), we give the dependences of the probe field and the second-order sideband on the driving power P_l for $\kappa > 0$. We see that these two processes are complementary at the resonance $\Delta_p = 0$: with decreasing P_l from 933 μW to 200 μW , the transmission rate of the probe field is slightly decreased, which results in a significant increasing of the second-sideband efficiency at $\Delta_p = 0$.

Fig. 3 shows the group delays of the transmitted probe field and the generated up-converted sideband signal in such an active COM system. For a conventional lossy cavity, only the slow-light effect can be observed for the probe field, while the second-order sideband experiences a slow-to-fast light transition at $P_l \sim 0.12$ mW. The relative delay between the two signals, $\Delta\tau_g = \tau_g - \tau'_g$, can be calculated for both cases of $\kappa > 0$ and $\kappa < 0$ (see Fig. 3(c)). We see that in the passive COM, $\Delta\tau_g > 0$, i.e. the probe field always travels behind the associated second-order sideband signal. However, the relative delay ($\sim 4\mu\text{s}$) is almost unchanged within a wide range of P_l , which is not beneficial for their separation in the time domain. In contrast, for the active COM system, the gain-assisted fast light can be observed for both the probe field and the second-order output signal, and the delay or advance can be significantly amplified by tuning κ and P_l . The maximum value of $\Delta\tau_g$ can be improved for about 25 times, in a similar range of P_l . Even the sign of $\Delta\tau_g$ can be reversed to negative at lower pump power, i.e. the second-order

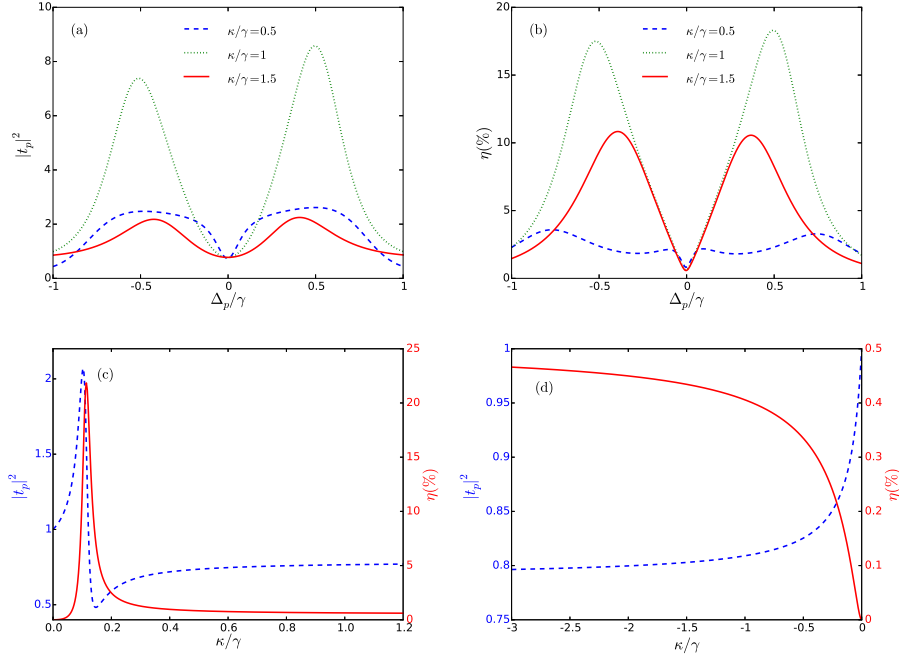


Fig. 4. (a,b) Transmission spectra of the probe field and the second-order sideband in an active-passive compound system, for $\kappa/\gamma=0.5$ (blue dashed), 1.0 (green dotted) and 1.5 (red solid). (c,d) $|t_p|^2$ (blue dashed) and η (red solid) at the resonance $\Delta_p = 0$, as a function of the gain-to-loss ratio κ/γ . In all the figures we have taken $J/\gamma = 1$ and $P_l = 933 \mu\text{W}$.

signal can also travel behind the probe field, which is strikingly distinct from the passive COM situation. This feature holds the promise to be useful for making e.g. a low-power modulator both in frequency and time domains.

3.2. Compound system with gain-loss balance

Now we probe the nonlinear OMIT in active-passive-coupled resonators (see Fig. 1(b)). First, as shown in Figs. 4(a,b), we give the transmitted spectra of the probe field and the efficiency of the second-order sideband for different values of $\kappa > 0$. For comparison, we have reproduced the results of Ref. [47] in Fig. 4(a). We find that for the off-resonance case $\Delta_p \neq 0$, the second-order profile shows an interesting similarity to the first-order case: the field amplification tends to be maximized as the gain and loss approach to the balance ($\kappa/\gamma = 1$), and the reversed-gain dependence works for both of the two processes.

In order to receive some analytical estimations, we take $\omega_m/\omega_c \sim 0$, $x_s \sim 0$, which approximately leads to

$$\eta \approx \left| \frac{i\hbar^2 g^4 |a_{1,s}|^2 a_{1,s}^* \kappa^4 \gamma \epsilon_p}{2m^2 \Gamma_m^2 \omega_m^3 (J^2 - \kappa\gamma)^3 [m\omega_m \Gamma_m (J^2 - \kappa\gamma) + i\hbar g^2 |a_{1,s}|^2 (J^2 - \kappa^2)]} \right|. \quad (14)$$

Obviously, in the vicinity of the gain-loss balance ($\kappa/\gamma = 1$, $J/\gamma = 1$), the efficiency of second-order sideband generation is most preferable. We also note that, at the resonance $\Delta_p = 0$, η is maximized for $\kappa/\gamma \sim 0.12$ (see Fig. 4(c)), still about 45 times of that in a passive COM system (see Fig. 4(d)).

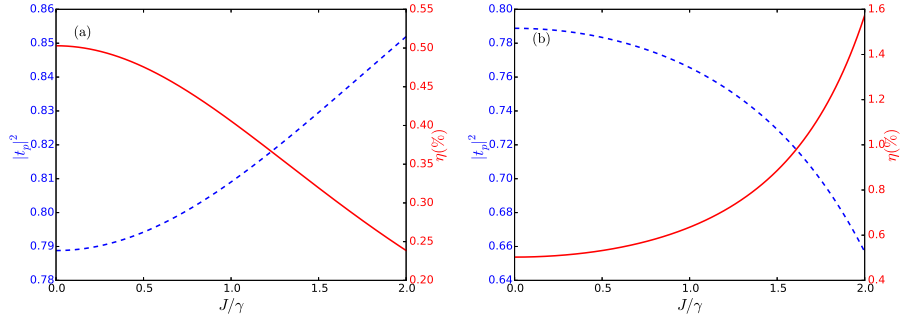


Fig. 5. Tuning the values of $|t_p|^2$ (blue dashed) and η (red solid) at $\Delta_p = 0$ by varying the tunneling rate J/γ , for the passive-passive case ($\kappa/\gamma = -1$) (a) or the active-passive case ($\kappa/\gamma = 1$) (b). The fixed value of the pump power is taken here as $P_l = 933 \mu\text{W}$.

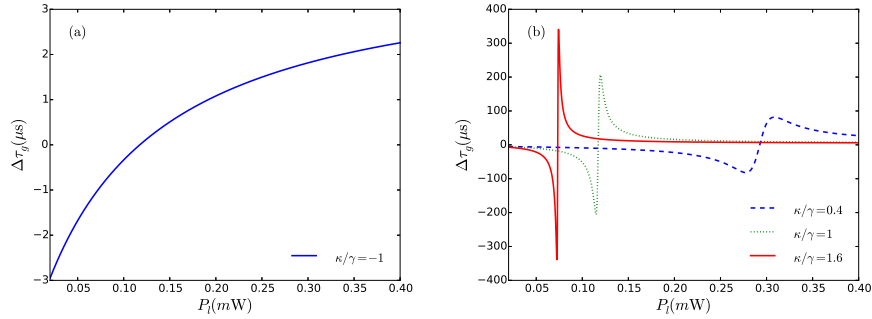


Fig. 6. The relative group delay $\Delta\tau_g$ as a function of P_l for the passive-passive system ($\kappa/\gamma = -1$) (a) or the active-passive system, with $\kappa/\gamma = 0.4$ (blue dashed), 1.0 (green dotted) and 1.6 (red solid) (b). Other parameters are $\Delta_p = 0$ and $J/\gamma = 1$.

For completeness, Fig. 5 illustrates the role of the optical tunneling rate J on both $|t_p|^2$ and η , at the resonance $\Delta_p = 0$. For $J/\gamma \rightarrow 0$, the compound system is reduced to the passive single-cavity system. We find that for the passive-passive system, stronger tunneling J is favorable for the first-order process (but not for the second-order process, see Fig. 5(a)) [30]; in contrast, for the active-passive system, stronger tunneling J is favorable for the second-order process (see Fig. 5(b)). Hence, with respect to a single-cavity device (at $\Delta_p = 0$), using a passive compound device leads to nearly half reduction of η , while using a gain-assisted compound device leads to a 3-fold enhancement under the same conditions.

Finally, Fig. 6 shows the relative delay between the probe and sideband fields for different COM systems (for the gain-assisted advance of the probe field, see Ref. [47]). For a passive-passive system with $\kappa/\gamma = -1$, $\Delta\tau_g$ only changes within the scope of several microseconds. In contrast, drastic changes of $\Delta\tau_g$ from delay to advance can be seen in the active-passive COM system, for example, up to $\pm 100 \mu\text{s}$ can be achieved for $\kappa/\gamma = 0.4$. In short, the active-passive COM can significantly strengthen the ability to modulate the linear and nonlinear responses of the system induced by the optomechanical interactions, particularly the ability to engineer their relative group delay or advance.

4. Conclusion

In summary, we have studied the transparency and the group-delay engineering of the probe field and the second-order sideband by considering the nonlinear optomechanical coupling in the active COM (single and compound systems). In the presence of strong pumping, the second-order sideband manifests itself as an inverted-OMIT spectrum, similar to the probe field. The efficiency of the second-order sideband process can be significantly enhanced in the vicinity of gain-loss balance for an active-passive compound COM system. We further analysis the ability of the active optomechanical systems for engineering the temporal sequence of both the probe and the sideband fields, i.e. their relative group delay or advance, which can be realized by varying the pump power and the gain. Our results provide new insights on active optomechanics in achieving multi-sideband optical transmission and temporal separation, which is potentially useful in optical information processing techniques. In the future, we plan to study the nonlinear OMIT processes in a cascaded system with two coupled mechanical modes [24], a hybrid COM system with an intracavity atom [13], or in an active COM system with an external mechanical driving [50].

Acknowledgements

We thank Xin-You Lü for helpful discussions. This work is supported partially by the CAS 100-Talent program and the National Natural Science Foundation of China under Grant numbers 11274098, 11474087, and 11422437.